CHIN. PHYS. LETT. Vol. 36, No. 6 (2019) 060501

A Three-Terminal Quantum Well Heat Engine with Heat Leakage *

Ze-Bin Lin(林泽斌), Wei Li(李唯), Jing Fu(符婧), Yun-Yun Yang(杨赟赟), Ji-Zhou He(何济洲)**
Department of Physics, Nanchang University, Nanchang 330031

(Received 3 January 2019)

We propose a model for a three-terminal quantum well heat engine with heat leakage. According to the Landauer formula, the expressions for the charge current, the heat current, the power output and the efficiency are derived in the linear-response regime. The curves of the power output and the efficiency versus the positions of energy levels and the bias voltage are plotted by numerical calculation. Moreover, we obtain the maximum power output and the corresponding efficiency, and analyze the influence of the heat leakage factor, the positions of energy levels and the bias voltage on these performance parameters.

PACS: 05.70.−a, 73.50.Lw, 73.63.Hs, 85.80.Fi DOI: 10.1088/0256-307X/36/6/060501

There has been increasing interest in developing highly efficient and powerful three-terminal nanoscale thermoelectric devices.[1−5] They involve ideal energy selective tunnel filters,[6,7] quantum dots,[8−13] quantum wells[14] and superlattices.[15] However, most of the previous works have not taken into account the heat leakage between the hot and cold reservoirs. The main focus in this study is to analyze the thermodynamic performance of a three-terminal quantum well thermoelectric heat engine with heat leakage. We discuss the optimal performance of the heat engine at maximum power output and the influence of the heat leakage on the performance of the heat engine in detail.

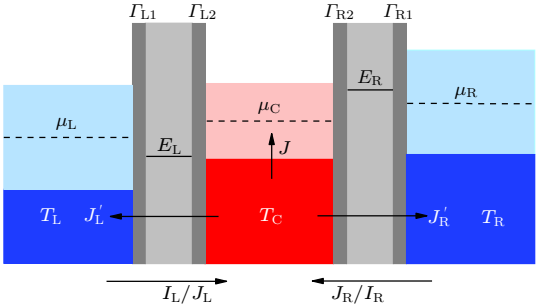

Fig. 1. Schematic diagram of a three-terminal heat engine based on quantum well. A central cavity (red) is connected to left/right electron reservoir with temperature T_i (i=L, R) and chemical potential μ_i (blue) via quantum wells (gray), and the central cavity with temperature T_C and chemical potential μ_C. The positive direction of the charge and heat currents is indicated by arrows.

The model we consider is schematically illustrated in Fig. 1. It consists of a central cavity connected via quantum wells to left and right electron reservoirs with temperature T_i (i=L ,R). The central cavity is kept at temperature T_C by a hot thermal reservoir. The temperatures of the left and right reservoirs are the same and lower than that of the central cavity ($T_L = T_R < T_C$). When no bias voltage is applied, the chemical potential μ_L/μ_R of the left/right electron reservoir is equal to the chemical potential μ_C of the central cavity. For simplicity, when a bias voltage V is applied, we take $\mu_L = -eV/2$ and $\mu_R = +eV/2$ (e is electronic charge). The chemical potential μ_C of the cavity is determined by the conservation of charge current, i.e., $I_L + I_R = 0$. The positive direction of the charge and energy currents is from reservoir i into the cavity. Based on the Landauer formula, the charge and energy currents can be evaluated by[14]

$$I_i = \frac{em^*A}{2\pi^2\hbar^3}\iint dE_\perp dE_Z T_i(E_Z)[f_i(E_Z+E_\perp) - f_C(E_Z+E_\perp)], \quad (1)$$

$$J_i = \frac{m^*A}{2\pi^2\hbar^3}\iint dE_\perp dE_Z (E_Z+E_\perp)T_i(E_Z) \cdot [f_i(E_Z+E_\perp) - f_C(E_Z+E_\perp)], \quad (2)$$

where $f_i = [\exp[(E_Z+E_\perp-\mu_i)/k_BT_i]+1]^{-1}$ is the Fermi distribution of reservoir i, $f_C = [\exp[(E_Z+E_\perp-\mu_C)/k_BT_C]+1]^{-1}$ is the Fermi distribution of the cavity, E_Z is the longitudinal component of electron energy parallel to the direction of transport, $E_\perp$ is the transverse component of electron energy perpendicular to it, k_B is the Boltzmann constant, m^* is the effective electron mass, A is the surface area of the quantum well, $\hbar$ is the Planck constant, and $T_i(E_Z)$ is the transmission function of the quantum well i,

$$T_i(E_Z) = \frac{\Gamma_{i1}(E_Z)\Gamma_{i2}(E_Z)}{(E_Z-E_i)^2 + [\Gamma_{i1}(E_Z)+\Gamma_{i2}(E_Z)]^2/4}, \quad (3)$$

with E_i being the resonant energy level within the quantum well i, $\Gamma_{i2}(E_Z)$ and $\Gamma_{i1}(E_Z)$ being the coupling strength of the quantum well i to the cavity and reservoir i, respectively.

In linear response, we introduce the temperature difference $\Delta T = T_C - T_i$ and average temperature $T = (T_C+T_i)/2$. The charge current and the heat current injected from the hot thermal reservoir can be given by

$$I = I_L = -I_R = GV + GS\Delta T, \quad (4)$$

$$J = -J_L - J_R = G\Pi V + (GS\Pi + H_1 + H_2)\Delta T, \quad (5)$$

where G and S are the electrical conductance and the

*Supported by the National Natural Science Foundation of China under Grant No 11365015.
**Corresponding author. Email: hjzhou@ncu.edu.cn
© 2019 Chinese Physical Society and IOP Publishing Ltd

Seebeck coefficient, respectively[15]

$$G = -\frac{e^2 m^* A}{2\pi^2\hbar^3}\frac{G_{\rm L1}G_{\rm R1}}{G_{\rm L1}+G_{\rm R1}},$$
$$S = \frac{k_{\rm B}}{e}\Big[\frac{G_{\rm L2}+G_{\rm L3}}{G_{\rm L1}} - \frac{G_{\rm R2}+G_{\rm R3}}{G_{\rm R1}}\Big],$$

and the auxiliary functions are

$$\Pi = \frac{k_{\rm B}T}{e}\Big[\frac{G_{\rm R2}+G_{\rm R3}}{G_{\rm R1}} - \frac{G_{\rm L2}+G_{\rm L3}}{G_{\rm L1}}\Big],$$
$$H_1 = -\frac{m^* A}{2\pi^2\hbar^3}k_{\rm B}^2 T\Big[\frac{(G_{\rm R2}+G_{\rm R3})^2}{G_{\rm R1}} + \frac{(G_{\rm L2}+G_{\rm L3})^2}{G_{\rm L1}}\Big],$$
$$H_2 = \frac{m^* A}{2\pi^2\hbar^3}k_{\rm B}^2 T[(G_{\rm L4}+2G_{\rm L5}-2G_{\rm L6}) + (G_{\rm R4}+2G_{\rm R5}-2G_{\rm R6})],$$
$$G_{i1} = \int_0^\infty dE_z T_i(E_z)\frac{1}{1+e^{E_z/k_{\rm B}T}},$$
$$G_{i2} = \int_0^\infty dE_z T_i(E_z)\frac{E_z/k_{\rm B}T}{1+e^{E_z/k_{\rm B}T}},$$
$$G_{i3} = \int_0^\infty dE_z T_i(E_z)\log(1+e^{-E_z/k_{\rm B}T}),$$
$$G_{i4} = \int_0^\infty dE_z T_i(E_z)\frac{(E_z/k_{\rm B}T)^2}{1+e^{E_z/k_{\rm B}T}},$$
$$G_{i5} = \int_0^\infty dE_z T_i(E_z)(E_z/k_{\rm B}T)\log(1+e^{-E_z/k_{\rm B}T}),$$
$$G_{i6} = \int_0^\infty dE_z T_i(E_z){\rm Li}_2(-e^{-E_z/k_{\rm B}T}).$$

In thermoelectric devices, the heat current is carried not only by the electrons, but also by the phonons. Based on a similar method,[15] we derive the phonon heat current from the central cavity

$$J_i' = A\int_{E_Z^-}^{E_Z^+}\frac{dE_Z}{h}E_Z\Delta F(E_Z, T_{\rm C}, T_i), \tag{6}$$

where $\Delta F(\omega(q_z), T_{\rm C}, T_i) = \int_{-\pi/d}^{+\pi/d}\frac{dq_x dq_y}{(2\pi)^2}[B_{\rm C}(\boldsymbol{q}) - B_i(\boldsymbol{q})]$ is a modified occupation difference, $B_{i/{\rm C}}(\boldsymbol{q}) = \{\exp[\hbar\omega(\boldsymbol{q})/k_{\rm B}T_{i/{\rm C}}] - 1\}^{-1}$ is the Bose–Einstein distribution of the reservoir (cavity), $E_Z = \hbar\omega(q_z)$ is the phonon energy of the longitudinal transport direction, $E_Z^{-(+)}$ is the minimum (maximum) phonon energy of the longitudinal transport direction, $q_{x(y)}$ is the transverse wave vector, q_z is the longitudinal wave vector, and d is the width of the quantum well. If the dispersion relation $\omega(\boldsymbol{q})$ is known, we may calculate the effective distribution $F(\omega(q_z))$ theoretically, then obtain the phonon heat current. However, this is generally a complicated issue. In the high-temperature limit $\hbar\omega(\boldsymbol{q})/k_{\rm B}T \ll 1$, we can simplify the phonon heat current to the following general form

$$J_i' = \kappa_i A\Delta T, \tag{7}$$

where κ_i is the thermal conductance coefficient, which is dependent on the width of the quantum well and the property of the quantum well material and is called the heat leakage. In the symmetric thermal conductance coefficient case ($\kappa_{\rm L} = \kappa_{\rm R} = \kappa$) the phonon heat current from the central cavity to the left/right reservoir is the same, i.e., $J_{\rm L}' = J_{\rm R}'$. Then after considering the phonon heat current we obtain the total heat current based on Eqs. (1)–(7) and the energy conservation law in the cavity

$$\begin{aligned} J &= -J_{\rm L} - J_{\rm R} + J_{\rm L}' + J_{\rm R}' \\ &= G\Pi V + (GS\Pi + H_1 + H_2)\Delta T + 2\kappa A\Delta T. \end{aligned} \tag{8}$$

The power output is

$$P = |IV| = |G|(V + S\Delta T)V, \tag{9}$$

which is independent of the phonon heat current, thus the efficiency is given by

$$\eta = P/J. \tag{10}$$

At $V = 0$, a finite charge current driven by the temperature difference $\Delta T \neq 0$ flows in a direction which depends on the position of the energy levels. When $E_{\rm R} > E_{\rm L}$, the direction of the charge current will be from the left reservoir to the right one. At $I = 0$, $V_{\rm stop} = -S\Delta T$ is called the stopping voltage where the heat-driven current is exactly compensated for by the bias-driven current flowing in the opposite direction.

In the following numerical calculation, we consider the asymmetry between the coupling strength of the left and the right quantum well, i.e., $\Gamma_{\rm L} = (1+a)\Gamma$ and $\Gamma_{\rm R} = (1-a)\Gamma$, where a satisfies the bounds $-1 \leqslant a \leqslant 1$, and Γ is the total coupling strength. Setting the average temperature $T = 300\,{\rm K}$ and the asymmetry $a = -0.5$, $\Gamma = 0.01k_{\rm B}T$, $\lambda = 2\kappa\pi\hbar^3/(k_{\rm B}m^*\Gamma)$ is defined as the heat leakage factor dependent on the total coupling strength and the thermal conductance coefficient, and $\eta_{\rm C}$ is the Carnot efficiency. Due to the high-temperature limit $\Delta T/T \ll 1$, $\eta_{\rm C} = \Delta T/T_{\rm C} \approx \Delta T/T$. The power output P is in units of $\frac{m^* A\Gamma}{2\pi\hbar^3}(k_{\rm B}\Delta T)^2$.

According to Eqs. (9) and (10), we plot three-dimension (3D) projection graphs of the power output P and the efficiency $\eta/\eta_{\rm C}$ varying with the positions of the two energy levels $E_{\rm L}$ and $E_{\rm R}$ at different heat leakage factors λ, as shown in Fig. 2. Since $eV = 1.5k_{\rm B}\Delta T > 0$, the working region is concentrated in the regions of $E_{\rm L} < 0$ and $E_{\rm R} > 0$. In Fig. 2(a), the maximum power output appears approximately at $E_{\rm L} = -5.5k_{\rm B}T$ and $E_{\rm R} = 1.5k_{\rm B}T$, which is independent of the heat leakage factor λ. However, the maximum values of the efficiency decrease and the maximum efficiency occur in smaller regions of $E_{\rm L}$ and $E_{\rm R}$ as the heat leakage factor increases, as shown in Figs. 2(b)–2(d). When the heat leakage factor is large enough (such as $\lambda = 10k_{\rm B}T$), the maximum power output and the maximum efficiency almost occur at the same position of the two energy levels.

Similarly we plot the curves of the power output P and the efficiency $\eta/\eta_{\rm C}$ versus the bias voltage eV at different heat leakage factors λ for given $E_{\rm R} = 1.5k_{\rm B}T$ and $E_{\rm L} = -5k_{\rm B}T$, as shown in Fig. 3. It is seen in

Fig. 3(a) that the power output firstly increases and then decreases as the bias voltage eV increases and is a symmetric parabola-like curve. However, the efficiency decreases as the heat leakage factor λ increases and is an asymmetric parabola-like curve, as shown in Fig. 3(b).

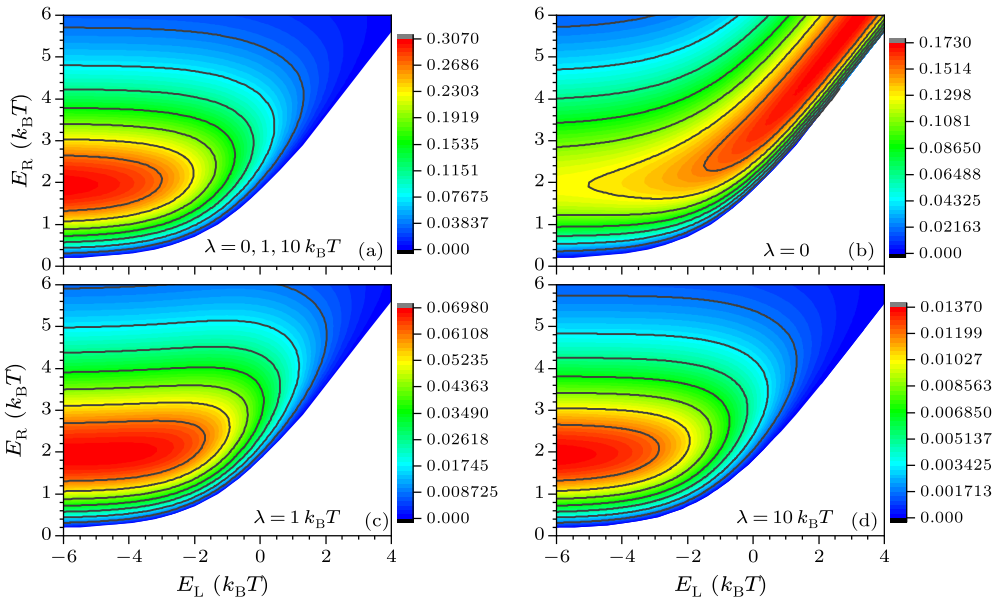

Fig. 2. (a) The power output versus the energy level (E_L, E_R), and (b)–(d) the efficiency versus the energy level (E_L, E_R) at different heat leakage factors λ for given $eV = 1.5k_B\Delta T$.

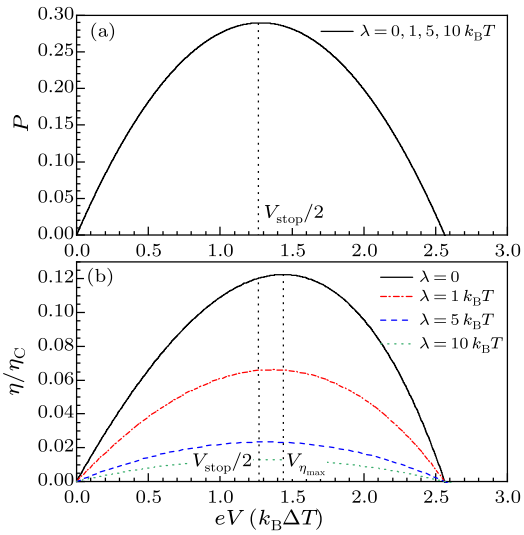

Fig. 3. (a) The power output P versus the bias voltage V. (b) The efficiency η/η_C versus the bias voltage V at different heat leakage factors λ. Here $E_L = -5k_BT$, $E_R = 1.5k_BT$ are given.

Using Eqs. (9) and (10) and the extremal condition

$$\frac{\partial P}{\partial V} = 0, \tag{11}$$

we can derive the expressions of the maximum power P_{max}, the corresponding efficiency $\eta_{max\,P}$ and the corresponding bias voltage $(V)_{mP}$, i.e.,

$$P_{max} = \frac{1}{4}|G|(S\Delta T)^2, \tag{12}$$

$$\eta_{max\,P} = \left|\frac{GS^2T}{GS\Pi + 2H_1 + 2H_2}\right|\frac{\eta_C}{2}, \tag{13}$$

$$V_{mp} = -\frac{1}{2}S\Delta T = \frac{1}{2}V_{stop}. \tag{14}$$

These optimal parameters all depend on the position of the energy levels and the heat leakage factor. Equations (13) and (14) are similar to the universal efficiency at maximum power in linear response derived by Broeck.[16] According to Eqs. (12) and (13), we plot the 3D projection graph of the maximum power output P_{max} and the corresponding efficiency $\eta_{max\,P}/\eta_C$ varying with the positions of the two energy levels E_L and E_R at different heat leakage factors λ, as shown in Fig. 4.

In Fig. 4(a), when $E_R \approx 1.5k_BT$ and $E_L \leqslant -5k_BT$, the maximum power output is approximately $P_{max} = 0.30$, which is independent of the heat leakage factor. For example, using $m^* = 0.067m_e$, $\Gamma = k_BT$, $T = 300\,K$, $\Delta T = 1\,K$, we obtain $P_{max} = 0.19\,W/cm^2$. Hence, the maximum power output of the quantum well heat engine is nearly twice that of a quantum dot heat engine,[11] but in Fig. 4(b)–4(d) the maximum value of the corresponding efficiency decreases from $\eta_{max\,P} \approx 0.16\eta_C$ to $\eta_{max\,P} \approx 0.012\eta_C$ as the heat leakage factor increases from $\lambda = 0$ to $\lambda = 10k_BT$. When sufficient heat from the hot reservoir is provided, reducing the heat leakage through quantum wells is a significant issue. For the position of the energy levels which maximize the power output, the corresponding efficiency decreases from $\eta_{max\,P} \approx 0.14\eta_C$ to $\eta_{max\,p} \approx 0.015\eta_C$ as the heat leakage factor increases from $\lambda = 0$ to $\lambda = 10k_BT$. This efficiency is much smaller than the efficiency at maximum power output of a quantum dot heat engine, which is given by $\eta_{max\,P} \approx 0.2\eta_C$.[11] The reason is that the quan-

tum dot only lets electrons of a special energy pass. In contrast, the quantum wells can transmit electrons of any energy larger than the resonant energy level $E_{\rm L}$ or $E_{\rm R}$, because any energy can be expressed as $E_Z + E_\perp$. Thus provided that E_Z matches the resonant energy, the electrons of any energy, even high-energy electrons, can pass through the quantum well. Therefore, the quantum wells are a much less efficient energy filter than quantum dots.

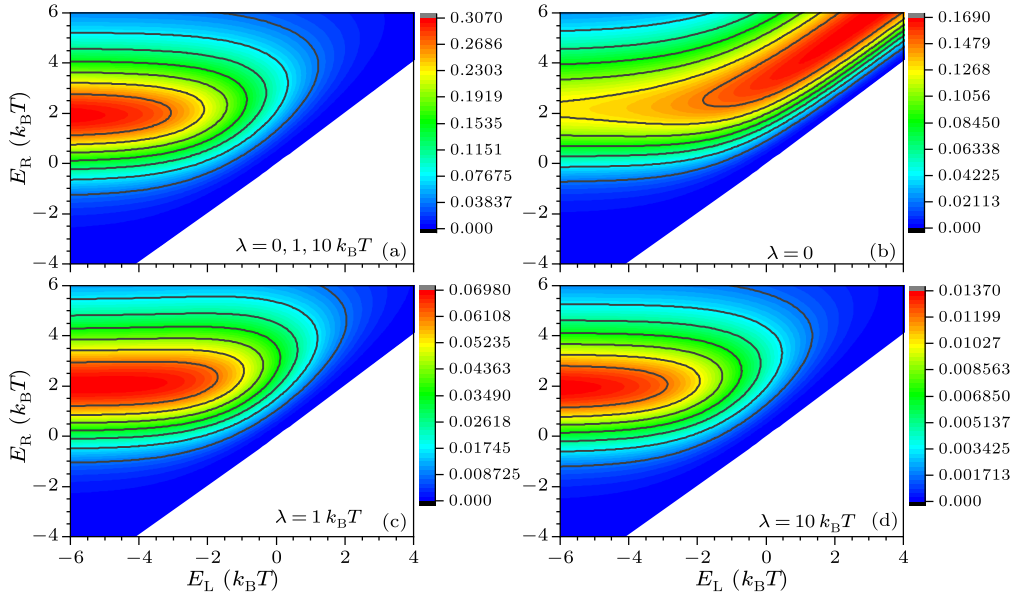

Fig. 4. (a) The maximum power output versus the energy level ($E_{\rm L}$, $E_{\rm R}$), and (b)–(d) the corresponding efficiency versus the energy level ($E_{\rm L}$, $E_{\rm R}$) at different heat leakage factors λ.

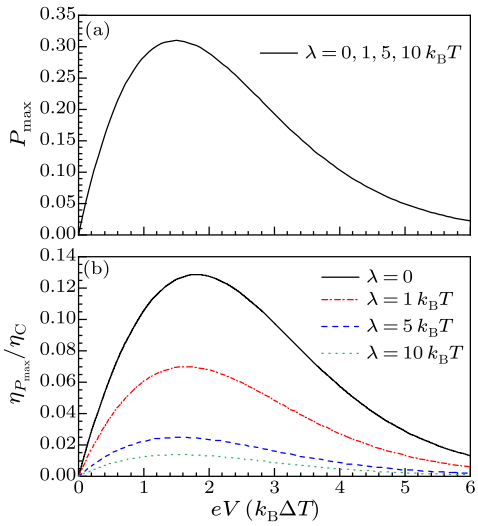

Fig. 5. (a) The maximum power output $P_{\rm max}$ versus the bias voltage, and (b) the efficiency at maximum power $\eta_{{\rm max}\,P}$ versus the bias voltage at different heat leakage factors λ.

Using Eqs. (9) and (10) and the extremal conditions

$$\frac{\partial P}{\partial E_{\rm L}} = 0, \text{ and } \frac{\partial P}{\partial E_{\rm R}} = 0, \tag{15}$$

we can numerically calculate the maximum power output $P_{\rm max}$, the corresponding efficiency $\eta_{{\rm max}\,P}$ and the corresponding energy levels $(E_{\rm L})_{\rm mp}$ and $(E_{\rm R})_{\rm mp}$. The curves of the maximum power output and the corresponding efficiency at the maximum power output are plotted as a function of the bias voltage at different heat leakage factors λ, as shown in Fig. 5.

It is found from Fig. 5 that the maximum power output $P_{\rm max}$ firstly increases then decreases as the bias voltage increases and reaches its maximum value at $eV \approx 1.5 k_{\rm B}\Delta T$. The corresponding efficiency largely decreases as the heat leakage factor increases, and the corresponding bias voltage at maximum efficiency also slightly decreases with the heat leakage factor. Thus to obtain the optimal performance parameters one should reduce the heat leakage factor as much as possible.

The main results obtained are as follows: (1) The phonon heat leakage significantly affects the performance parameters of the quantum well heat engine. Thus the phonon heat leakage needs to be considered in analyzing the performance of the heat engine. (2) The quantum wells are a much less efficient energy filter than quantum dots. Thus the power output of the quantum well heat engine is larger than that of the quantum dot heat engine, but its efficiency is smaller than that of the quantum dot heat engine.

References

[1] Benenti G et al 2017 *Phys. Rep.* **694** 1
[2] Sothmann B et al 2015 *Nanotechnology* **26** 032001
[3] Thierschmann H et al 2015 *Nat. Nanotechnol.* **10** 854
[4] Roche B et al 2015 *Nat. Commun.* **6** 6738
[5] Josefsson M et al 2018 *Nat. Nanotechnol.* **13** 920
[6] Su H et al 2015 *Chin. Phys. Lett.* **32** 100501
[7] Su S et al 2016 *Sci. Rep.* **6** 21425
[8] Edwards H L et al 1993 *Appl. Phys. Lett.* **63** 1815
[9] Edwards H L et al 1995 *Phys. Rev. B* **52** 5714
[10] Prance J R et al 2009 *Phys. Rev. Lett.* **102** 146602
[11] Jordan A N et al 2013 *Phys. Rev. B* **87** 075312
[12] Shi Z C et al 2017 *Chin. Phys. Lett.* **34** 110501
[13] Kano S and Fujii M 2017 *Nanotechnology* **28** 095403

[14] Sothmann B et al 2013 *New J. Phys.* **15** 095021
[15] Choi Y and Jordan A N 2015 *Physica E* **74** 465
[16] Van Den Broeck C 2005 *Phys. Rev. Lett.* **95** 190602